

Maximum Power Point Tracking Control of Wind Turbine Generators Based on High-order Torque Curve

Liansong Guo, Zaiyu Chen, *Member, IEEE*, Minghui Yin, *Member, IEEE*, Chenxiao Cai, *Senior Member, IEEE*, and Yun Zou, *Member, IEEE*

Abstract—The optimal torque (OT) method, which is preferred for its simplicity, is widely employed in maximum power point tracking (MPPT) control strategies for wind energy capture in wind turbine generators (WTGs). Based on the OT method, the decreased torque gain (DTG) method is developed to improve turbine acceleration through a reduction of the torque gain coefficient. However, the DTG method does not fully align with the acceleration performance required by wind turbines, which subsequently limits improvements in wind energy capture efficiency. To address these concerns, a novel MPPT control strategy is proposed, which introduces redefined torque curve and torque command conceptualized based on a higher-order function relative to rotor speed. Additionally, an adaptive algorithm for the periodic update of the torque command is suggested to better accommodate the variability of turbulent wind speeds, thus aiming to improve the wind energy capture efficiency. The effectiveness of the proposed MPPT control strategy is substantiated through the wind turbine simulator (WTS)-based experiments.

Index Terms—Maximum power point tracking (MPPT) control, optimal torque (OT), decreased torque gain (DTG), high-order torque, wind turbine generator (WTG).

NOMENCLATURE

λ	Tip speed ratio (TSR)
λ_{opt}	Optimal TSR
γ	Compensation coefficient
σ	Stress amplitude
$\omega_{opt}^{v_a+\Delta v}$	Optimal speed at wind speed $v_a + \Delta v$ (rad/s)
$\omega_{eDTG}^{v_a+\Delta v}$	Steady-state rotor speed at wind speed $v_a + \Delta v$ using decreased torque gain (DTG) method (rad/s)

ω_r	Rotor speed (rad/s)
$\dot{\omega}_r$	Rotor speed acceleration (rad/s ²)
ω_{ri}	Rotor speed at the i^{th} sample (rad/s)
$\Delta\omega_{diff}$	Difference of steady-state rotor speed between DTG and optimal torque (OT) methods (rad/s)
ρ	Air density (kg/m ³)
σ_j	Stress amplitude
v	Wind speed (m/s)
v_i	Wind speed at the i^{th} sample (m/s)
β	Pitch angle (°)
C_p	Power coefficient
C_{pmax}	The maximum power coefficient
J_t	Total inertia of wind turbine generator (WTG) equivalent to low-speed shaft (kg·m ²)
m_j	Number of cycles of σ_j
M	Number of generator torque distribution intervals
n	Number of samples
p	Gain coefficient
P_e	Electric power output (kW)
P_{favg}	Wind energy capture efficiency
$\Delta P_{DTG}^{loss}, \Delta P_{HOT}^{loss}$	Losses for wind energy capture using DTG and higher-order torque (HOT) methods (kW)
q	Gain exponent
Q_a, Q_b, Q_c, Q_d	Different operation states of wind turbine
R	Radius of wind rotor (m)
Δt	Sampling interval (s)
$\Delta t_{OT}, \Delta t_{DTG}$	Time required to attain the maximum power point (MPP) of WTG using optimal torque (OT), DTG, and HOT methods after sudden surge in wind speed (s)
Δt_{HOT}	Time required to attain the maximum power point (MPP) of WTG using optimal torque (OT), DTG, and HOT methods after sudden surge in wind speed (s)
$\Delta T_{dOT}, \Delta T_{dDTG}$	Unbalanced torques of WTG using OT, DTG, and HOT methods (kN·m)
ΔT_{dHOT}	Unbalanced torques of WTG using OT, DTG, and HOT methods (kN·m)
T_e	Generator torque of WTG at low-speed shaft (kN·m)
T_{eOT}, T_{eDTG}	Generator torques of WTG using OT, DTG, and HOT methods (kN·m)
T_{eHOT}	Generator torques of WTG using OT, DTG, and HOT methods (kN·m)

Manuscript received: April 12, 2024; revised: June 4, 2024; accepted: June 14, 2024. Date of CrossCheck: June 14, 2024. Date of online publication: July 15, 2024.

This article is distributed under the terms of the Creative Commons Attribution 4.0 International License (<http://creativecommons.org/licenses/by/4.0/>).

This work was supported in part by the National Key R&D Program of China (No. 2021YFB1506904) and the National Natural Science Foundation of China (No. 51977111).

L. Guo, Z. Chen, M. Yin (corresponding author), C. Cai, and Y. Zou are with the School of Automation, Nanjing University of Science and Technology, Nanjing 210094, China (e-mail: liansguo@126.com; zaiyu.chen@njust.edu.cn; ymhui@vip.163.com; ccx5281@njust.edu.cn; zouyun@njust.edu.cn).

DOI: 10.35833/MPCE.2024.000395



T_{ei}	Generator torque of WTG at the i^{th} sample (kN·m)
ΔT_{eDTG}	Difference in generator torque of WTG between OT and DTG methods (kN·m)
ΔT_{eHOT}	Difference in generator torque of WTG between OT and HOT methods (kN·m)
T_g	Generator torque of WTG (kN·m)
$T_{g,\text{cmd}}$	Torque command of WTG (kN·m)
T_r	Aerodynamic torque of WTG (kN·m)
ΔT_r	Variation in aerodynamic torque of WTG (kN·m)

I. INTRODUCTION

THE recent surge in interest towards renewable and clean energy sources has spotlighted the potential of wind energy [1]–[3]. The maximum power point tracking (MPPT) control strategies [4], [5], which maximize the wind energy capture efficiency for wind turbine generators (WTGs), are pivotal in this regard. There are several methods including the optimal torque (OT) method [6], tip speed ratio (TSR) method [7], and perturb and observe (P&O) method [8], which form the basis of MPPT control strategies. The OT method is extensively used in engineering applications due to its operational convenience and low transmission chain load [9], [10]. This study focuses on enhancing the performance of WTG using the OT method.

In essence, the OT method is a systematic steady-state-based control method. It utilizes the maximum power point (MPP), i.e., the steady-state operating point at different wind speeds, to derive the OT curve. Subsequently, the MPPT is realized by adjusting the generator torque of WTG through rotor speeds. However, as the capacity of WTGs and rotor inertia progressively increase, the slow dynamics of WTGs are intensified, leading to significant tracking losses and a decline in wind energy capture efficiency at turbulent wind speeds in [11].

To elevate the discourse surrounding the optimization of wind turbines, recent investigations foreground the enhanced methodologies predicated on the OT method, including the following:

1) The decreased torque gain (DTG) method [12], which attenuates the gradient of the generator torque curve via the incorporation of a torque gain coefficient, thereby diminishing generator torque and enhancing the acceleration performance.

2) The reduction of tracking range (RTR) method [13] and effective tracking range (ETR) method [14], which eliminate segments of the torque curve and abbreviate the tracking range of WTG for wind gusts, thereby improving the wind energy capture efficiency.

3) The inertia compensation control (ICC) method [15], [16], constant bandwidth control (CBC) method [17], [18], and optimally tracking rotor (OTR) method [10]. A generator torque compensation term is added to increase the torque discrepancy. Furthermore, an adaptive compensation control method is developed to dynamically adjust the compensation

term [11].

Among these methods, the DTG method distinguishes itself with its simple principle and extensive deployment in engineering practices. Notably, by merely attenuating the incline of the torque curve, the generator torque of WTG in the DTG framework remains a function solely dependent on rotor speed [12], [19]. It ensures that the deviations in the generator torque of WTG are minimally exacerbated, thereby harmonizing enhancements in wind energy capture efficiency with the mitigation of augmented drive-train loads.

Given that the DTG method encompasses an adjustable gain coefficient which exerts an influence on wind energy capture efficiency, current academic efforts predominantly focus on fine-tuning this aspect of the DTG method so as to optimize its performance.

Based on the DTG method, the adaptive torque control (ATC) [20] method is developed to periodically adjust the DTG gain coefficient at different wind speeds. To overcome the problem of the nonconvergence for searching the coefficient under turbulence, an improved adaptive-torque gain MPPT control is proposed in [21]. Furthermore, the convergence speed of the gain coefficient is improved in [22]. Different from the searching method, an optimized DTG method is proposed to optimize the gain coefficient offline, which is more adaptable to the turbulent wind speeds [23]. Nonetheless, these methods steadfastly adhere to the structural confines of the DTG method.

This study finds that, due to the adherence to the form of the torque curve, the extent to which the DTG method reduces generator torque that positively correlates with wind speed. This leads to the difficulty in improving the acceleration performance of WTG to adapt to changes in wind speed. This limitation is particularly evident in the following operational aspects:

1) At low wind speeds, the aerodynamic torque weakens, so there is a greater necessity to reduce the generator torque significantly to increase the unbalanced torque. However, the DTG method only marginally reduces the generator torque, resulting in a limited increase in unbalanced torque. This limitation hampers the effectiveness of improving the acceleration performance and wind energy capture efficiency of WTGs.

2) At high wind speeds, the significantly amplified aerodynamic torque predominates the amplitude of the unbalanced torque. However, the DTG method markedly diminishes the generator torque at high wind speeds. The powerful aerodynamic torque in conjunction with the significantly weakened generator torque leads to a significant surge in the unbalanced torque. This results in excessive turbine acceleration and consequently reduces wind energy capture efficiency.

To circumvent these challenges, a redefined torque curve based on a higher-order function (greater than 2) relative to rotor speed and torque command is proposed in this study, substituting the traditional quadratic function utilized in the DTG method. It allows the reduction in generator torque to be inversely correlated with the rotor speed, which effectively creates a negative association between the generator

torque reduction and wind speed.

Furthermore, an adaptive algorithm is proposed, which can dynamically modify the torque command parameters at turbulent wind speeds. The tracking capability can be effectively enhanced at low wind speeds. In addition, issues related to excessive acceleration can be mitigated at high wind speeds. Thus, the proposed adaptive algorithm strives to improve the wind energy capture efficiency. The effectiveness of the proposed MPPT control strategy is substantiated through the wind turbine simulator (WTS)-based experiments. The major contributions of this study are summarized as follows.

1) It is found that the DTG method enhances the acceleration performance of WTGs in a manner misaligned with their operational needs. Specifically, it falls short in boosting the acceleration of WTGs at low wind speeds, where enhancement is critically needed for WTGs, and conversely amplifies acceleration excessively at high wind speeds. Both outcomes detract from improving the wind energy capture efficiency.

2) A redefined torque curve and a torque command are proposed, which are finely attuned to the acceleration requirements of WTGs. They significantly elevate the acceleration performance at low wind speeds and mitigate the risk of undue acceleration at high wind speeds.

3) An adaptive algorithm for adjusting torque command parameters in response to fluctuating wind speeds is proposed. By fine-tuning curve parameters dynamically, the proposed adaptive algorithm thereby adapts better to different wind speeds.

4) The proposed adaptive algorithm not only effectively improves wind energy capture efficiency but also ensures its simplicity and ease of application, which harmonizes the engineering effectiveness with practical viability.

The rest of this study is organized as follows. Section II introduces the modeling of WTG and review of the OT and DTG methods. Section III discusses the acceleration performance of WTG using DTG method at different wind speeds. Section IV proposes the proposed MPPT control strategy. Section V presents the experimental validation. Finally, Section VI provides conclusions.

II. MODELING OF WTG AND REVIEW OF OT AND DTG METHODS

The block diagram of permanent-magnet synchronous generator (PMSG)-type WTG with MPPT control strategy is shown in Fig. 1. It mainly includes two dynamic processes of the realization of the MPPT control, which are mechanical dynamics and electromagnetic dynamics. The mechanical dynamics encompass elements, i.e., the rotor blades and gearbox, while the electromagnetic dynamics comprise the generator, converter, and grid. The MPPT control strategy can adjust the rotor speed of WTGs by modulating the generator torque through the torque command $T_{g,cmd}$.

Given the disparity in response time between the mechanical (significantly longer) [24] and electromagnetic dynamics, electromagnetic dynamics can be considered to have an in-

stantaneous response when discussing mechanical dynamics. Because this study focuses on mechanical dynamics in conjunction with MPPT control, the methodology in this paper is predicated on the presumption that generator control can swiftly and accurately fulfill the electric torque command through the idea of fast-slow dynamic decoupling, i.e., $T_g = T_{g,cmd}$ [25].

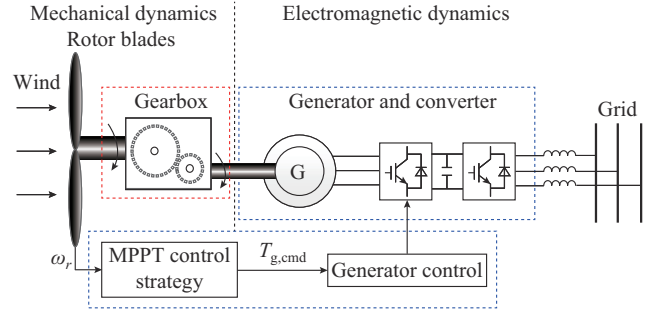


Fig. 1. Block diagram of PMSG-type WTG with MPPT control strategy.

A. Modeling of WTG

The aerodynamic power captured by a WTG is defined as P_r , which is given as [12]:

$$P_r = \frac{1}{2} \rho \pi R^2 v^3 C_p(\lambda, \beta) \quad (1)$$

$$\lambda = \frac{\omega_r R}{v} \quad (2)$$

Generally, the pitch angle β remains fixed for MPPT control, i.e., $\beta=0$. In this case, $C_p(\lambda, \beta)$ can be considered a function only of λ . A typical power coefficient curve is depicted in Fig. 2. This curve manifests as a single-peak function, thereby identifying an optimal TSR λ_{opt} , which maximizes C_p (denoted as C_{pmax}). Notably, both λ_{opt} and C_{pmax} are contingent upon the structural design of WTG and may vary across different turbines.

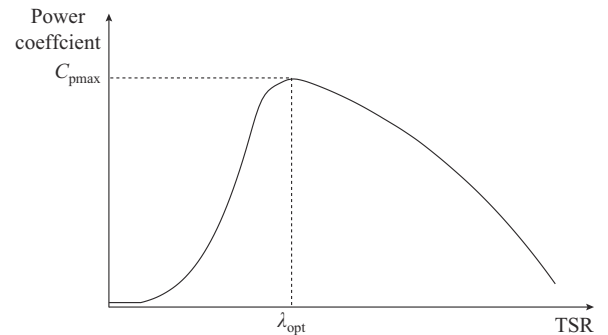


Fig. 2. Typical power coefficient curve.

Assuming a perfectly rigid shaft and ignoring the damping coefficients, the mechanical dynamics can be simplified as [26]:

$$J_t \dot{\omega}_r = T_r - T_e = \frac{P_r - P_e}{\omega_r} \quad (3)$$

B. Review of OT and DTG Methods

Figure 3 shows the aerodynamic power curve at different

wind speeds. When the wind speed is v_a , the aerodynamic power curve against the rotor speed is $P_r(v_a, \omega_r)$. When the WTG operates at the optimal rotor speed ω_a , corresponding to the optimal TRS λ_{opt} , C_p reaches its peak C_{pmax} , as shown in Fig. 2. At the operating state point $Q_a(\omega_a, v_a)$, P_r achieves its maximum value P_{max} .

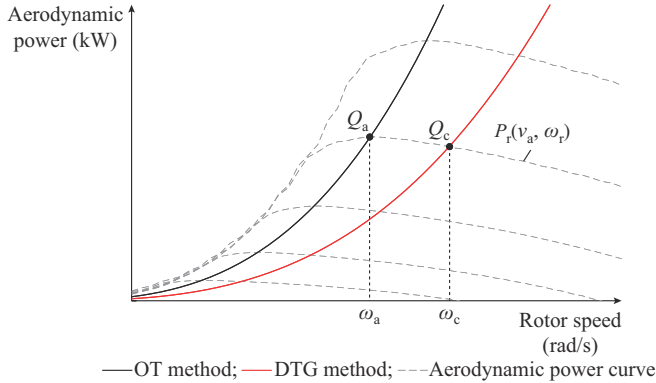


Fig. 3. Aerodynamic power curve at different rotor speeds.

As shown in Fig. 3, by connecting these MPPs at different wind speeds, the generator torque of WTG using the OT method is constructed as:

$$T_{eOT} = K_{opt} \omega_r^2 \quad (4)$$

where $K_{opt} = \rho \pi R^5 C_{pmax} / (2 \lambda_{opt}^3)$ is approximately constant.

The rotor speed can gradually converge towards the optimal speed through (4), which ultimately facilitates the attainment of MPPT.

However, due to the substantial inertia of the WTG, the acceleration and deceleration of the rotor speed are relatively sluggish at different wind speeds. This substantial inertia makes it challenging for the WTG to consistently operate at the MPP, causing losses in wind energy capture efficiency [27], which becomes more pronounced at low wind speeds due to insufficient aerodynamic torque.

In the face of these challenges, researchers direct their attention towards improving the dynamic performance of WTGs, which may lead to the development of the DTG method. Building upon the framework of OT method, the generator torque of WTG using the DTG method can be expressed as:

$$T_{eDTG} = \alpha K_{opt} \omega_r^2 \quad (5)$$

where $\alpha \in (0, 1)$.

When $\alpha < 1$, there is $T_{eDTG} < T_{eOT}$ at the identical rotor speeds. Through (3), it leads to a more significant rotor speed acceleration $\dot{\omega}_r$ when tracking gradual wind gusts. As a result, the DTG method enhances the tracking abilities of WTGs, thereby bolstering their wind energy capture efficiency [12], [27]. The engineering principle behind the DTG method is simple and widely applicable, making it a suitable topic for further improvement and analysis in this study.

Significantly, the DTG method leverages a fixed value for α and suggests an approximate range of α in [6], [12], and [19]. Subsequent studies indicate that the optimal value of α usually depends on different wind speeds, which improves

the wind energy capture efficiency [6]. Therefore, the ATC method is proposed to dynamically adjust the parameter α according to complex wind conditions [12], [20]. The aim of the ATC method is to further improve the wind energy capture efficiency. Current studies primarily concentrate on adjusting the parameter α dynamically based on the torque curve to contend with different wind speeds [24], [28]. The improvements in the form of the torque curve itself are often overlooked. However, this study specifically investigates and proposes advancements in this aspect.

III. ACCELERATION PERFORMANCE OF WTG USING DTG METHOD AT DIFFERENT WIND SPEEDS

Taking step-changed wind speeds as a representative example, this section delves into the variable characteristics of the unbalanced torque at different wind speeds. The acceleration performance of WTG using the DTG method at different wind speeds is subsequently explored.

A. Components for Unbalanced Torque

The unbalanced torque, which comprises both T_r and T_e components, has a significantly influences on the acceleration performance of WTGs. By comparing the unbalanced torque between OT and DTG methods at different wind speeds, the enhancement in acceleration performance of WTG using the DTG method can be evaluated.

Generated from (3), the unbalanced torque ΔT_d can be denoted as:

$$\Delta T_d = T_r - T_e \quad (6)$$

Assuming that the current wind speed is v_a , when the turbine is at the steady-state operating point (i.e., MPP), the steady-state rotor speed is $\omega_a = \lambda_{opt} v_a / R$ (i.e., the optimal rotor speed of v_a) using the OT method. Therefore, we denote the steady-state operating point as $Q_a(\omega_a, v_a)$. At this time, the unbalanced torque ΔT_d equals 0, i.e.,

$$T_{eOT}(\omega_a) = T_r(v_a, \omega_a) \quad (7)$$

When the wind speed abruptly increases Δv , the rotor speed cannot instantaneously adjust and remains at ω_a due to the inertia of the rotor. As a result, the variation in the aerodynamic torque component amounts to:

$$\Delta T_r = T_r(v_a + \Delta v, \omega_a) - T_r(v_a, \omega_a) \quad (8)$$

When using the OT method, it is confirmed that the generator torque stays constant during an instantaneous wind speed variation from (4). Hence, ΔT_{eOT} can be given as:

$$\Delta T_{eOT} = T_r - T_e = T_r(v_a, \omega_a) + \Delta T_r - T_{eOT}(\omega_a) = \Delta T_r \quad (9)$$

Figure 4 shows the components of unbalanced torque of WTG using the DTG method. Equation (9) signifies that under the variation of Δv , the turbine encounters an unbalanced torque of ΔT_r . It means that the acceleration performance of WTG using the OT method is solely determined by ΔT_r , as illustrated in Fig. 4.

In contrast, the value of generator torque of WTG using the DTG method at Q_a is $T_{eDTG}(\omega_a)$ from (5), which can be obtained as:

$$T_{eDTG}(\omega_a) = T_{eOT}(\omega_a) - \Delta T_{eDTG} \quad (10)$$

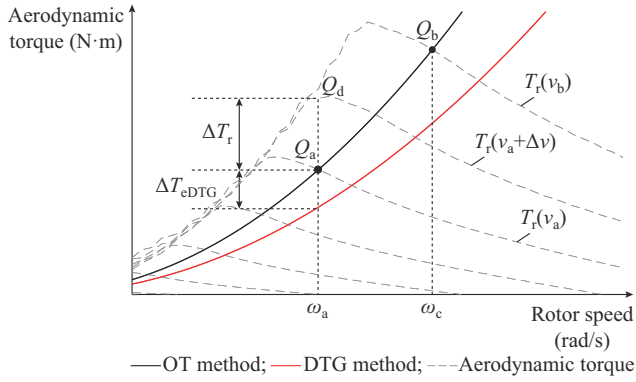


Fig. 4. Components of unbalanced torque of WTG using DTG method.

When upon the variation of Δv at Q_a , the variation in aerodynamic torque of WTG using the DTG method aligns with that using the OT method, i.e., ΔT_r . Hence, the unbalanced torque of WTG using the DTG method is:

$$\Delta T_{\text{dDTG}} = T_r - T_c = T_r(v_a, \omega_a) + \Delta T_r - T_{\text{eDTG}}(\omega_a) = \Delta T_r + \Delta T_{\text{eDTG}} \quad (11)$$

It can be observed that the unbalanced torque of WTG using the DTG method at a step-changed wind speed comprises two components: ΔT_r and ΔT_{eDTG} , as illustrated in Fig. 4. At an identical step-changed wind speed, the unbalanced torque of WTG using the DTG method surpasses that using the OT method, which shows a superior acceleration performance.

Note 1: to analyze the unbalanced torque of WTG using the DTG method at different wind speeds, the OT method is taken as a reference. Both DTG and OT methods select the same operating point, specifically the MPP, which coincidentally is also the steady-state operating point of WTG using the OT method. In the subsequent text, unless otherwise stated, the steady state refers to the steady-state operating point of WTG using the OT method, i.e., MPP.

B. Positive Correlation Between Unbalanced Torque Components and Wind Speed

The acceleration performance of WTG using the DTG method is determined by both ΔT_r and ΔT_{eDTG} . Therefore, the acceleration performance at different wind speeds can be ascertained by comparing ΔT_r and ΔT_{eDTG} at different steady-state operating points.

1) Correlation Between ΔT_r and v

Performing small-signal analysis [18] at $Q_a(\omega_a, v_a)$, the variation in aerodynamic torque in the vicinity of $Q_a(\omega_a, v_a)$ can be described by:

$$\Delta T_r(v, \omega) = \left. \frac{\partial T_r}{\partial v} \right|_{Q_a} \Delta v + \left. \frac{\partial T_r}{\partial \omega_r} \right|_{Q_a} \Delta \omega_r \quad (12)$$

Considering the rotor speed cannot respond to the abrupt alteration of the wind speed instantaneously, the variation in rotor speed is 0, i.e., $\Delta \omega_r = 0$. Hence, the variation in aerodynamic torque resulting from the wind speed variation $\Delta T_r|_{Q_a}$ is given as:

$$\Delta T_r|_{Q_a} = \frac{3\rho\pi R^3 C_{p\text{max}}}{2\lambda_{\text{opt}}} v_a \Delta v \quad (13)$$

Upon Δv at different steady-state operating points, i.e., $Q_b(\omega_b, v_b)$, where $v_b > v_a$ and $\omega_b > \omega_a$, there exists a difference of $\Delta T_r|_{Q_b}$ and $\Delta T_r|_{Q_a}$, which can be given as:

$$\Delta T_r|_{Q_b} > \Delta T_r|_{Q_a} \quad (14)$$

This implies that the value of ΔT_r is smaller at low wind speed v_a for the same value of Δv , resulting in a smaller unbalanced torque ΔT_d . Conversely, ΔT_r is larger at the high v_a , which leads to a larger ΔT_d .

2) Correlation Between ΔT_{eDTG} and v

Similarly, the difference in generator torque of the WTG at Q_a is given as:

$$\Delta T_{\text{eDTG}}|_{Q_a} = (1 - \alpha) K_{\text{opt}} \omega_a^2 \quad (15)$$

It can be observed that ΔT_{eDTG} is related to the steady-state rotor speed ω_a . In addition, ω_a correlates with the wind speed in a one-to-one relationship ($\omega_a \leftrightarrow v_a$) at the steady-state operating point. To analyze the characteristics of the unbalanced torque at different wind speeds, (15) can be written as:

$$\Delta T_{\text{eDTG}}|_{Q_a} = (1 - \alpha) K_{\text{opt}} \frac{\lambda_{\text{opt}}^2}{R^2} v_a^2 \quad (16)$$

Hence, the value of ΔT_{eDTG} is related to the current wind speed v_a at Q_a . For different steady-state operating points Q_a and Q_b , there is:

$$\Delta T_{\text{eDTG}}|_{Q_b} > \Delta T_{\text{eDTG}}|_{Q_a} \quad (17)$$

In summary, the variation in aerodynamic torque ΔT_r resulting from the same Δv amplifies as the wind speed v_a escalates. Additionally, an extra variation in ΔT_{eDTG} is also intensified at high wind speeds.

Note 2: this study primarily concentrates on the relationship between the unbalanced torque components at the step-changed wind speed and the wind speed at that moment, rather than its relationship with the magnitude of the change of the wind speed.

C. Improvement Effect on Acceleration Performance

The acceleration performance of WTGs can be evaluated by the duration taken to return to the MPP following the step-changed wind speed [29]. By comparing the discrepancy in this duration between OT and DTG methods at different wind speeds, the relationship between the improvement effect on acceleration performance of WTG using the DTG method and wind speed can be discerned.

The dynamic equation of the WTG can be represented as:

$$\Delta \dot{\omega}_r = \frac{1}{J_t} \Delta T_d = \frac{1}{J_t} (\Delta T_r + \Delta T_{\text{eDTG}}) \quad (18)$$

From (9), ΔT_{dOT} equals ΔT_r . Thus, by substituting (9) into (18), we can obtain the time required to reach the MPP again at Q_a after a sudden increase in the wind speed Δv using the OT method, which is given as:

$$\Delta t_{\text{OT}} = \frac{2J_t \lambda_{\text{opt}}^2}{3\rho\pi R^4 C_{p\text{max}} v_a} \quad (19)$$

Since the acceleration performance of WTG using the OT method is determined by ΔT_r , and ΔT_r is larger along with the high wind speed, there is a greater acceleration resulting in a shorter time required to reach the MPP at the high wind speed.

Analogously, the time required to attain the MPP of WTG using the DTG method after a sudden increase in the wind speed Δv at Q_a is given as:

$$\Delta t_{\text{DTG}} = \frac{2J_t \lambda_{\text{opt}}^2 \Delta v}{\rho \pi R^4 C_{\text{pmax}} [3\Delta v + (1-\alpha)v_a] v_a} \quad (20)$$

Compared with the OT method, the unbalanced torque of WTG using the DTG method comprises not only ΔT_r but also ΔT_{eDTG} . Given that ΔT_r for various methods remains unaffected, it sustains its constancy for both methods at the same steady-state operating point and wind speed. Thus, the distinction between the OT and DTG methods in their acceleration performance hinges on ΔT_{eDTG} .

To symbolize the improvement effect of ΔT_{eDTG} on the acceleration performance, the ratio of the difference in acceleration time of WTG between OT and DTG methods is defined as $\delta t_{\text{OT,DTG}}$, which is given as:

$$\delta t_{\text{OT,DTG}} = \frac{\Delta t_{\text{OT}} - \Delta t_{\text{DTG}}}{\Delta t_{\text{OT}}} = \frac{(1-\alpha)v_a}{3\Delta v + (1-\alpha)v_a} \quad (21)$$

A larger value of $\delta t_{\text{OT,DTG}}$ signifies a shorter duration required to reach the MPP compared with the OT method, resulting in superior enhancement of the acceleration performance of WTG using the DTG method.

Comparing $\delta t_{\text{OT,DTG}}$ at different steady-state operating points, we can obtain:

$$\delta t_{\text{OT,DTG}}|_{Q_a} < \delta t_{\text{OT,DTG}}|_{Q_b} \quad (22)$$

Formula (22) reveals that the improvement effect on the acceleration performance of WTG using the DTG method escalates with the increase of wind speed.

Compared with that at high wind speeds, the acceleration performance of WTG using the OT method is inferior at low wind speeds. Under such circumstances, it is crucial to significantly enhance the acceleration performance of WTG at low wind speeds. However, the improvement effect on the acceleration performance cannot be enhanced effectively when using the DTG method. In other words, the issue of low wind energy capture efficiency due to weak acceleration performance is not effectively solved.

Note 3: the DTG method includes mutually corresponding acceleration performance and deceleration performance of WTG, whereby the improvement effect on the acceleration performance equals the decrease in deceleration performance during deceleration.

D. Over-acceleration Phenomenon

From the above-mentioned analysis, there is an improvement effect on acceleration performance of WTG using the DTG method at high wind speed. In fact, the improvement effect is accompanied by a deviation at the operating point. As a consequence, the WTGs continue to accelerate even reaching the new MPP. Ultimately, the turbine deviates from the optimal rotor speed, which results in a reduction in wind

energy capture efficiency. Especially, the severity of this over-acceleration phenomenon increases with the increase in wind speed.

The dynamic equation of WTG using the DTG method is symbolized as:

$$J_t \dot{\omega}_r = T_r - \alpha K_{\text{opt}} \omega_r^2 \quad (23)$$

Denote the steady-state rotor speed at $v_a + \Delta v$ for DTG as $\omega_{\text{eDTG}}^{v_a + \Delta v}$. Let $\dot{\omega}_r = 0$, and $\omega_{\text{eDTG}}^{v_a + \Delta v}$ can be given as:

$$\omega_{\text{eDTG}}^{v_a + \Delta v} = \zeta \frac{(v_a + \Delta v) \lambda_{\text{opt}}}{R} \quad (24)$$

$$\zeta = \left(\frac{\alpha C_{\text{pmax}}}{C_p(\lambda_c)} \right)^{-\frac{1}{3}} \quad (25)$$

where λ_c is a constant and $\lambda_c > \lambda_{\text{opt}}$.

Figure 5 shows the rotor speed trajectory at step-changed wind speeds. When $0 < \alpha < 1$, it is evident that $\omega_{\text{eDTG}}^{v_a + \Delta v} > \omega_{\text{opt}}^{v_a + \Delta v}$. As depicted in Fig. 5, the WTG begins to accelerate at time t_0 when the wind speed abruptly increases from v_a to $v_a + \Delta v$. It maintains this acceleration until the WTG hits the optimal rotor speed $\omega_{\text{opt}}^{v_a + \Delta v}$ at time t_1 and subsequently reaches a steady-state rotor speed $\omega_{\text{eDTG}}^{v_a + \Delta v}$ at time t_2 . The difference between the optimal rotor speed at wind speed $v_a + \Delta v$ and the steady-state rotor speed at wind speed $v_a + \Delta v$ using the DTG method is defined as:

$$\Delta \omega_{\text{diff}} = \omega_{\text{eDTG}}^{v_a + \Delta v} - \omega_{\text{opt}}^{v_a + \Delta v} \quad (26)$$

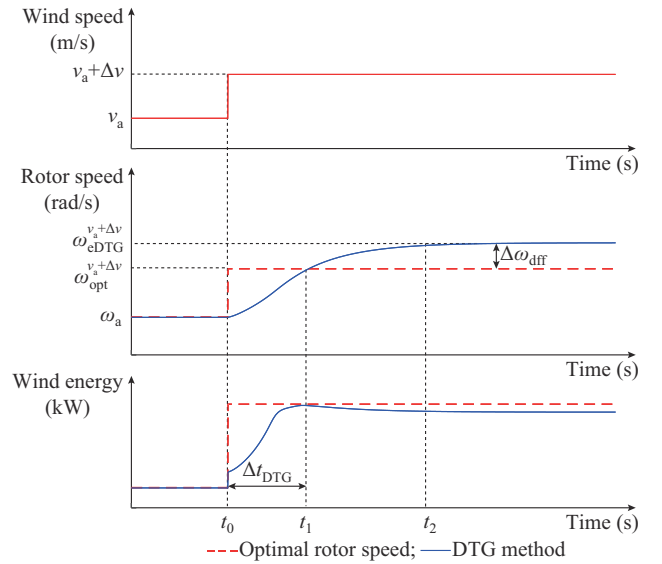


Fig. 5. Rotor speed trajectory at step-changed wind speeds.

Given that the WTG does not operate at the MPP upon reaching $\omega_{\text{eDTG}}^{v_a + \Delta v}$ when using the DTG method, the wind energy that can be captured at $\omega_{\text{eDTG}}^{v_a + \Delta v}$ falls short of the maximum wind energy that can be captured at $v_a + \Delta v$. The losses for the wind energy capture using the DTG method can be given as:

$$\Delta P_{\text{DTG}}^{\text{loss}} = \frac{1}{2} \rho \pi R^2 (v_a + \Delta v)^3 (C_{\text{pmax}} - C_p(\lambda_c)) \quad (27)$$

Figure 6 shows the steady-state rotor speed at different

wind speeds. Moreover, $\Delta\omega_{\text{diff}}$ is larger along with the high wind speed, as demonstrated in Fig. 6. This implies that the higher the wind speed, the greater the loss for the wind energy capture due to $\Delta\omega_{\text{diff}}$. In fact, considering the inadequate acceleration performance of WTGs, the reduction in wind energy capture efficiency owing to over-acceleration is seldom observed in the low wind speed spectrum. Moreover, the amount of wind energy harnessed at low wind speeds is relatively minimal, and even a minor fluctuation in rotor speed would not inflict substantial losses for wind energy capture. As such, the implications brought about by steady-state speed deviations only warrant the consideration at high wind speeds.

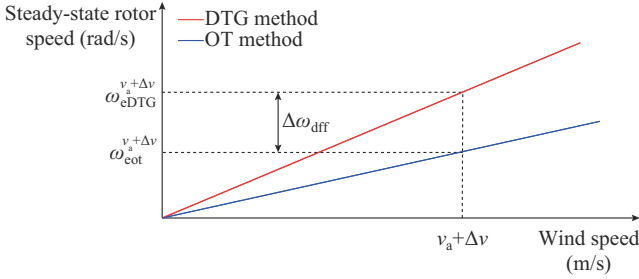


Fig. 6. Steady-state rotor speed at different wind speeds.

Therefore, we can draw the following conclusions.

1) At low wind speeds, it is necessary to enhance the acceleration performance of WTG due to its inherent aerodynamic properties, though the improvement effect on the acceleration performance of WTG using the DTG method is modest.

2) At high wind speeds, the over-acceleration phenomenon induced by the significantly heightened acceleration performance of WTG using the DTG method results in decreased wind energy capture efficiency.

Therefore, priority should be given to bolstering the acceleration performance of WTG at low wind speeds and mitigating the losses for wind energy capture prompted by significantly heightened acceleration at high wind speeds, which is the objective of this study.

IV. PROPOSED MPPT CONTROL STRATEGY

To tackle the issues of lackluster acceleration performance at low wind speeds and over-acceleration at high wind speeds when using the DTG method, this section explores a redefined torque curve of WTG using the HOT method. The HOT method aims to enhance the acceleration performance at low wind speeds while guaranteeing wind energy capture efficiency at high wind speeds, thereby further enhancing the wind energy capture efficiency. In this section, we denote the torque curve of WTG using the HOT, OT, and DTG methods as the HOT curve, OT curve, and DTG curve, respectively.

A. Design for HOT Curve

This subsection introduces the design for the HOT curve. Figure 7 shows the HOT curve at different rotor speeds. The generator torque of WTG using the HOT curve is given as:

$$T_{\text{eHOT}} = p\omega_r^q \quad q \geq 3, q \in \mathbb{N} \quad (28)$$

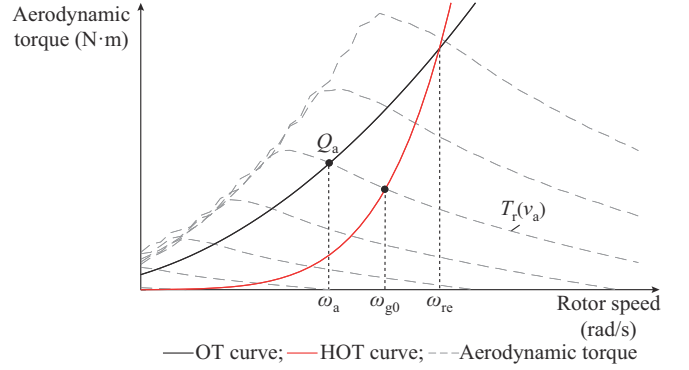


Fig. 7. HOT curve at different rotor speeds.

Assuming that ω_{re} is the intersection point of the generator torque curve and the OT curve, we can obtain p as:

$$p = K_{\text{opt}} \frac{1}{\omega_{re}^{q-2}} \quad (29)$$

In (28), the gain exponent q represents the degree of curvature of the torque curve. The larger the value of q , the more pronounced the curvature of the torque curve. When $q=2$, the torque curve can degenerate to the OT curve.

In (29), ω_{re} represents the upper limit of the interval for the improvement effect on the acceleration performance of WTG using the HOT method. When the rotor speed satisfies $\omega_r < \omega_{re}$, the unbalanced torque increases significantly. Thus, the acceleration performance of WTG can be effectively enhanced. From (29), it can be inferred that, when q is determined, the gain exponent p is determined by ω_{re} .

T_{eHOT} in (28) alters the form of the OT curve and causes a change in the steady-state operating point. Therefore, the stability of WTG using the HOT method is analyzed firstly before discussing the dynamic characteristics caused by the HOT curve.

Assuming a given constant wind speed v_a as the input, let $\dot{\omega}_r = 0$ and solve for the equilibrium speed at v_a as ω_{g0} . Taking the Lyapunov function as $V = \tilde{e}^2$, where $\tilde{e} = \omega_r - \omega_{g0}$, we obtain:

$$\dot{V} = \rho\pi R^2 v_a^2 (\lambda - \lambda_g) \left[\frac{C_p(\lambda)}{\lambda} - \frac{C_{p\text{max}}}{\lambda_{\text{opt}}^3} \left(\frac{\lambda_g}{\lambda_{re}} \right)^{q-2} \lambda_g^2 \right] \leq 0 \quad (30)$$

where $\lambda_{g0} = \omega_{g0} R / v_a$ holds if and only if $\lambda = \lambda_{g0}$; and $\lambda_{re} = \omega_{re} R / v_a$.

Therefore, the WTG at wind speed v_a is asymptotically stable. The rotor speed gradually approaches ω_{g0} with the provided initial speed.

Indeed, this study discards the traditional quadratic function form of the rotor speed commands and designs a HOT curve. As depicted in Fig. 7, the HOT curve has the following advantages.

1) It exhibits a higher degree of curvature at low wind speeds, which significantly increases the unbalanced torque of the WTG and enhances its acceleration performance.

2) It gradually approaches the OT curve at high wind speeds, reducing the unbalanced torque and ensuring that the WTG does not lose wind energy capture efficiency due to

the significantly heightened acceleration.

It is apparent that the control instruction of the torque curve in this study is also concise with strong engineering practicability.

B. Acceleration Performance of WTG Using HOT Method at Different Wind Speeds

For the HOT curve proposed in Section IV-A, the improvement effect on acceleration performance at different wind speeds is analyzed through the variation in generator torque at different wind speeds. Then, this subsection analyzes the acceleration performance of WTG using the HOT method at different wind speeds.

Firstly, similar to the analysis in Section III, the variation in generator torque at Q_a when the wind speed changes for HOT method can be defined as (31). We set $\gamma = v_a/v_{re}$, where v_{re} is the corresponding wind speed to ω_{re} at MPP, i.e., $v_{re} = \omega_{re}R/\lambda_{opt}$.

$$\Delta T_{eHOT}|_{Q_a} = T_{eOT}(\omega_a) - T_{eDTG}(\omega_a) = \frac{K_{opt}\lambda_{opt}^2}{R^2}(1 - \gamma^{q-2})v_a^2 \quad (31)$$

To investigate the improvement effect on acceleration performance of WTG using the HOT method at different wind speeds, that is, the variation characteristics of ΔT_{eHOT} at different steady-state operating points, we can obtain:

$$\left. \frac{\Delta(\Delta T_{eHOT})}{\Delta v} \right|_{Q_a} = \frac{K_{opt}\lambda_{opt}^2}{R^2}(2 - q\gamma^{q-2})v_a \quad (32)$$

$$\begin{cases} \left. \frac{\Delta(\Delta T_{eHOT})}{\Delta v} \right|_{Q_a} \geq 0 & 0 < v_a \leq \left(\frac{2}{q}\right)^{\frac{1}{q-2}} v_{re} \\ \left. \frac{\Delta(\Delta T_{eHOT})}{\Delta v} \right|_{Q_a} < 0 & v_a > \left(\frac{2}{q}\right)^{\frac{1}{q-2}} v_{re} \end{cases} \quad (33)$$

From (33), as the wind speed increases, ΔT_{eHOT} first accelerates rapidly and then gradually decelerates. Furthermore, it can be deduced that the time required for the WTG to reach the MPP again after a sudden increase in wind speed Δv from Q_a when using HOT method is:

$$\Delta t_{HOT} = \frac{2\lambda_{opt}^2 J_t \Delta v}{\rho \pi R^4 C_{pmax} [3\Delta v + (1 - \gamma^{q-2})v_a] v_a} \quad (34)$$

By defining the ratio of the difference in acceleration time of WTG between the OT and HOT methods as $\delta t_{OT,HOT}$, we can obtain:

$$\delta t_{OT,HOT} = \frac{\Delta t_{OT} - \Delta t_{HOT}}{\Delta t_{OT}} = \frac{(1 - \gamma^{q-2})v_a}{3\Delta v + (1 - \gamma^{q-2})v_a} \quad (35)$$

Equation (35) represents the improvement effect on acceleration performance of WTG using the HOT method. The larger the value of ΔT_{eHOT} , the stronger the improvement effect. It can be concluded as:

$$\begin{cases} \delta t_{OT,HOT} > \delta t_{OT,DTG} & 0 < v_a < \alpha^{\frac{1}{q-2}} v_{re} \\ \delta t_{OT,HOT} \leq \delta t_{OT,DTG} & v_a \geq \alpha^{\frac{1}{q-2}} v_{re} \end{cases} \quad (36)$$

Therefore, as shown in Fig. 8, the HOT method has the

following properties compared with the DTG method.

1) The low wind speeds ($0 < v_a < \alpha^{(q-2)^{-1}} v_{re}$) offer a greater improvement effect on acceleration performance, resulting in quicker acceleration.

2) At high wind speeds ($v_a \geq \alpha^{(q-2)^{-1}} v_{re}$), its improvement effect on acceleration performance is weaker than the DTG method, ensuring that the WTG may not lose wind energy capture efficiency due to excessive acceleration.

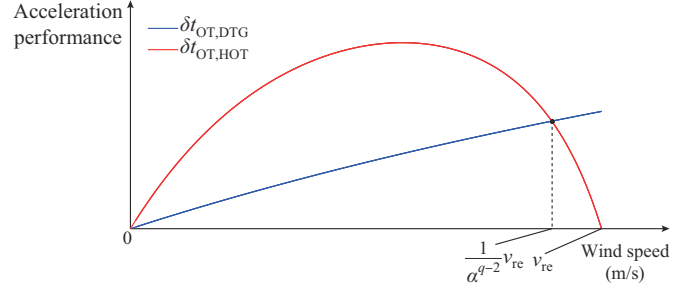


Fig. 8. Comparison of acceleration performance.

C. Parameter Tuning of HOT Method at Different Wind Speeds

As evident from (28), the control command proposed in this study includes two parameters, q and ω_{re} , which play a crucial role in influencing the wind energy capture efficiency. As detailed in Section IV-A, ω_{re} is particularly associated with the wind speed environment. In addition, it is ascertained that q does not affect the steady-state rotor speed.

Thus, this study does not consider the influence of the variation in parameter q on the dynamics of the WTG and initially establishes a constant value for q through empirical data. Setting $q=4$ leads to the following torque instruction, and we can obtain:

$$T_{eHOT} = K_{opt} \frac{1}{\omega_{re}^2} \omega_r^4 \quad (37)$$

Following the determination of q , a method is introduced for dynamically adjusting ω_{re} in response to the fluctuation of the wind speed.

As shown in Section III-D, the DTG method has a fixed $\Delta\omega_{diff}$ with the optimal speed. This often results in substantial losses for the wind energy capture at high wind speeds. In the HOT method, the deviation depends on the setting of ω_{re} . If the rotor speed converges to the optimal speed after a step change in the wind speed, it can prevent losses for the wind energy capture caused by significantly heightened acceleration. Thus, when $\omega_{re} = \omega_{eOT}^{v_a + \Delta v} = (v_a + \Delta v)\lambda_{opt}/R$, we can obtain:

$$\Delta P_{HOT}^{loss} = 0 \quad (38)$$

However, the set of accurate ω_{re} based on uncertain wind speed is challenging, especially during variable wind speeds, i.e., turbulence. Therefore, to minimize losses for the wind energy capture triggered by steady-state speed deviation at high wind speeds, this study periodically calculates and updates ω_{re} based on variation of wind speed.

We define n as the number of samples taken within period

$[t_k, t_{k+1}]$. The maximum wind energy captured within a period $[t_k, t_{k+1}]$ can be expressed as:

$$E_{\max k} = \frac{1}{2} \rho \pi R^2 C_{p\max} \sum_{i=1}^n v_i^3 \quad (39)$$

Thus, there exists v_k , which satisfies:

$$E_{\max k} = \frac{1}{2} \rho \pi R^2 n v_k^3 C_{p\max} \quad (40)$$

where $v_k \in [\min v_i, \max v_i]$ can be viewed as the equivalent wind speed value within period $[t_k, t_{k+1}]$ that maximizes the wind energy capture efficiency, that is:

$$v_k = \left(\frac{1}{n} \sum_{i=1}^n v_i^3 \right)^{\frac{1}{3}} \quad (41)$$

Let $\omega_k = v_k \lambda_{\text{opt}} / R$, and the equivalent rotor speed corresponding to the maximum wind energy capture efficiency within period $[t_k, t_{k+1}]$ can be obtained. If the wind energy capture efficiency reaches its maximum within period $[t_k, t_{k+1}]$, the average rotor speed $\bar{\omega}_{\text{Tu}}$ equals ω_k . Therefore, ω_{re} can be adjusted by calculating the difference $e = \bar{\omega}_{\text{Tu}} - \omega_k$, that is:

$$\omega_{\text{re}}^{k+1} = \omega_{\text{re}}^k + \gamma \text{sgn}(e)|e| \quad (42)$$

By using (42), the next value of ω_{re} within the next period can be determined. The flow chart of updating ω_{re} is shown in Fig. 9, where WTS is short for wind turbine simulator. Periodic updates of ω_{re} can enhance the wind energy capture efficiency at different wind speeds, particularly at variable wind speeds. The scheme of control strategy of HOT method is shown in Fig. 10.

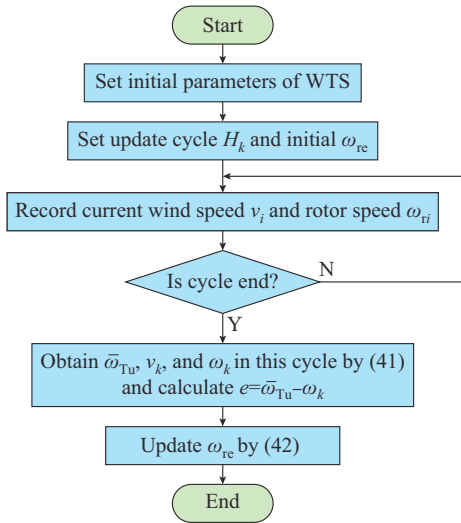


Fig. 9. Flow chart of updating ω_{re} .

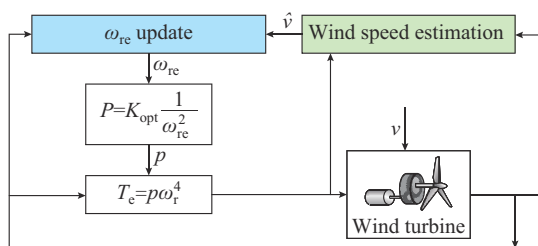


Fig. 10. Scheme of control strategy of HOT method.

Note 4: from the torque command in (28), it is observed that the gain exponent q also influences dynamic performance of WTGs by affecting the rate of change of generator torque. However, it is ascertained that q does not affect the steady-state rotor speed. Therefore, this study does not consider the influence of the variation in q on the dynamic performance of WTG and only provides a method for setting ω_{re} to adapt to variable wind speed.

V. EXPERIMENTAL VALIDATION

In this section, an experimental platform of a single-bus power system integrated with wind power is employed to validate the enhanced effectiveness of the proposed MPPT control strategy in improving the wind energy capture efficiency [30], [31]. The superiority of using HOT method is aimed to be thoroughly verified by comparing with the performance of WTG against the OT, ATC, and OTR methods at variable wind speeds.

A. WTS-based WTG Experimental Platform

The WTS-based WTG experimental platform of a single-bus power system integrated with wind power is constructed, which can emulate the mechanical dynamics of the 600 kW CART3 [32]. The WTS-based WTG experimental platform is depicted in Fig. 11, where PLC is short for programmable logic controller. The parameters of the wind turbine and the experimental platform are provided in Tables I and II, respectively [30]. The WTS-based WTG experimental platform includes the following three main parts.

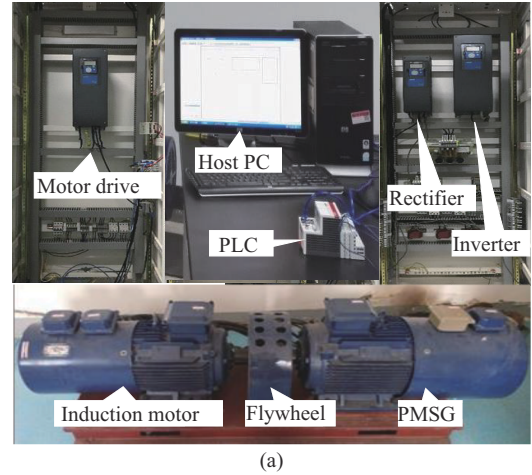


Fig. 11. WTS-based WTG experimental platform. (a) Laboratory setup for experimental testing. (b) Schematic diagram of WTS-based WTG test bench.

TABLE I
PARAMETERS OF WIND TURBINE

Parameter	Value
Number of blades	3
Rotor radius	20 m
Hub height	36.6 m
Rated power	600 kW
Gearbox ratio	43.165
Rated torque	3580 N·m
λ_{opt}	5.8
C_{pmax}	0.46

TABLE II
PARAMETERS OF WTG-BASED EXPERIMENTAL PLATFORM

Parameter	Value
Control period	40 ms
Rated power	15 kW
Rated speed	1500 r/min
Moment of inertia	0.72 kg·m ²
Rated voltage	380 V
Rated current	22 A

1) WTS: it consists of a motor drive, an induction motor, a flywheel, and the simulation program running in a PLC. The simulation program can accurately simulate the aerodynamic characteristics and the slow dynamics of the CART3 based on the fatigue, aerodynamics, structures, and turbulence (FAST) code and inertia compensation [31].

2) Electrical part: it includes a PMSG and a inverter. The rectifier controls the electromagnetic torque of the PMSG according to the torque command $T_{g,cmd}$ received from the PLC. This part is a real WTG.

3) MPPT controller: it is programmed in the PLC to implement various MPPT strategies. It sends the torque command $T_{g,cmd}$ to the rectifier in each control cycle.

B. Performance Metrics

To enable a quantitative assessment of the control effect across various methods, the following performance metrics are initially introduced.

1) The wind energy capture efficiency over a period can be expressed as:

$$P_{favg} = \frac{\sum_{i=1}^n (T_{ei}\omega_{ri} + J_r\omega_{ri}\dot{\omega}_{ri})\Delta t}{\sum_{i=1}^n \frac{1}{2} \rho \pi R^2 v_i^3 \Delta t} \quad (43)$$

In addition, we denote ΔP_{favg} as the difference of P_{favg} between OT method and other methods.

2) The damage equivalent load (DEL) [33] refers to the sinusoidal stress amplitude that can generate equivalent damage as the original signal at a constant frequency f during a certain period T , which is defined as:

$$DEL = \left(\sum_{j=1}^M \frac{\sigma_j^4 m_j}{Tf} \right)^{\frac{1}{4}} \quad (44)$$

Choose $Tf=1$. The lower the DEL value, the less the fluctuation in generator torque and the reduced drive-train loads.

C. Analysis of Experimental Results

There are four 60-min variable wind speed profiles applied in the experiments, which are generated by the commercial simulation software Bladed [34]. The turbulence class is *A* and the mean wind speed \bar{v} is 4, 5, 6, and 7 m/s, respectively. Choose one of the wind speed profiles as an example, as shown in Fig. 12. The statistics of performance metrics are listed in Table III, where the update cycle for ω_{re} is 600 s.

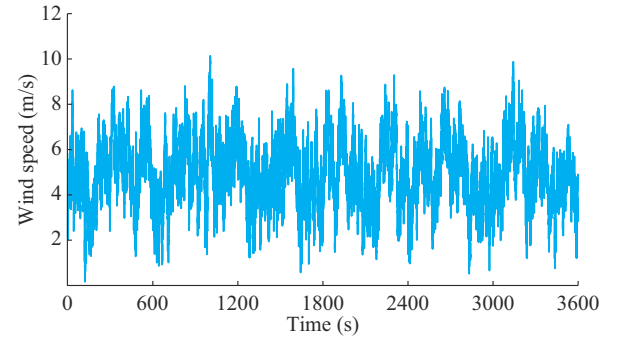


Fig. 12. Turbulent wind speed profiles applied in experiments ($\bar{v}=5$ m/s).

TABLE III
STATISTICS OF PERFORMANCE METRICS

\bar{v} (m/s)	Method	P_{favg} (%)	ΔP_{favg} (%)	DEL
4	OT	84.32		1.39
	ATC	89.05	4.73	1.39
	OTR	87.16	2.84	4.97
	HOT	92.44	8.12	1.85
5	OT	87.67		1.94
	ATC	91.01	3.34	1.94
	OTR	90.83	3.16	5.36
	HOT	93.22	5.55	2.56
6	OT	92.75		2.68
	ATC	93.87	1.12	2.66
	OTR	94.02	1.27	6.89
	HOT	94.88	2.13	3.52
7	OT	93.82		3.78
	ATC	94.45	0.63	3.74
	OTR	95.13	1.31	10.30
	HOT	95.20	1.38	4.80

1) Wind Energy Capture Efficiency of WTG

As delineated by the statistical data in Table III, the HOT method proposed in this study demonstrates a superior wind energy capture efficiency when compared with the ATC and OTR methods.

Indeed, with the implementation of the proposed MPPT control strategy, the WTG captures more wind energy at

high average wind speeds. This is because the WTG exhibits improved acceleration performance at these high average wind speeds with the increase in aerodynamic torque, which generates a stronger driving force on the rotor. Consequently, when using the OT method, there is a notable increase in wind energy capture efficiency as the wind speed increases.

However, at low wind speeds, the lack of adequate aerodynamic torque leads to suboptimal wind energy capture efficiency. In this situation, the exceptional capability of the HOT method to enhance wind energy capture efficiency becomes particularly evident. In essence, the lower the wind speed, the more pronounced the improvement in wind energy capture efficiency when using the HOT method.

2) Dynamic Characteristics of Rotor Speed

To analyze the impact on acceleration performance at variable wind speeds, rotor speed trajectories corresponding to the typical low wind speed range and typical high wind speed range are depicted in Figs. 13 and 14, respectively.

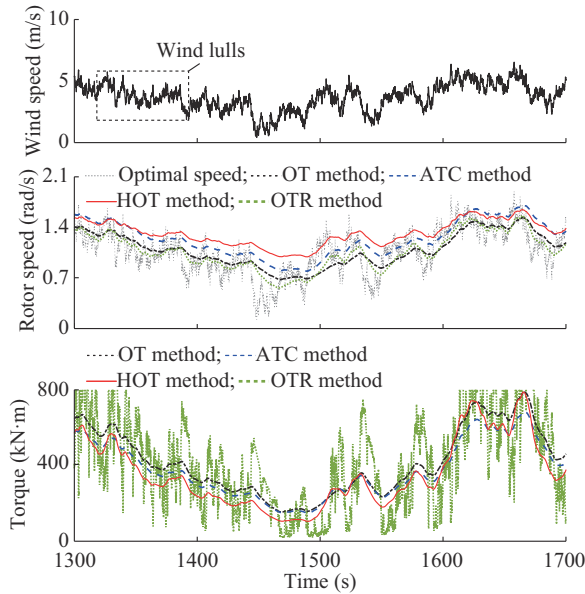


Fig. 13. Comparison of experimental results in typical low wind speed range.

In the low wind speed range, the rotor speed trajectory of WTG using the HOT method supersedes that using the other methods. In reality, the continuous fluctuation of variable wind speeds makes it difficult for the WTG to maintain steady-state speeds at different wind speeds. In such circumstances, the HOT method provides the WTG with strong acceleration performance against wind gusts and decreased deceleration performance against wind lulls at low wind speeds, enabling them to continuously operate at a speed above the rotor speed of WTG using other methods. This inevitably sacrifices a little wind energy capture efficiency to retain more kinetic energy for tracking increasing gusts.

In the high wind speed range, the rotor speed trajectory of WTG using the HOT method is significantly below that using the ATC method, and comparable to that using the OT method. Specifically, at high wind speeds with higher wind energy content, the HOT method no longer enhances the acceleration performance against gradually strengthening gusts.

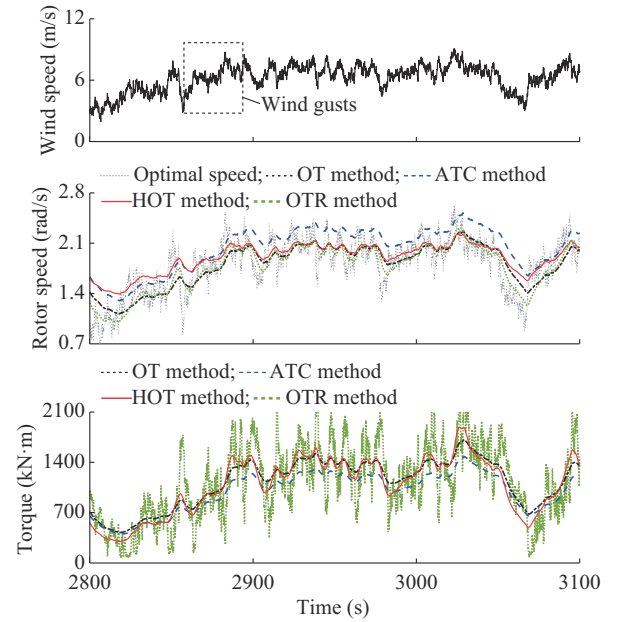


Fig. 14. Comparison of experimental results in typical high wind speed range.

This prevents the WTG from running at excessively high speeds, thereby ensuring the wind energy capture efficiency.

3) Drive-train Loads

The torque command of WTG using the HOT method is predicated upon the fourth power of speed, a notable divergence from the ATC method, which relies on the square of speed. This distinction broadens the range of generator torque fluctuations, consequentially precipitating an increase in load.

Despite this increase in load, it is critical to underscore that the generator torque curve remains a simplistic and smooth function exclusively dependent on rotor speed. It does not precipitate marked or frequent shifts in the generator torque. As shown in Table III, *DEL* using the HOT method is much smaller than that using the OTR method. Therefore, the magnitude of the increase in load is adjudged to be within acceptable limits. A salient benefit of the HOT method is its adeptness at circumventing undue increase in loads.

4) Impacts on Update Cycle of ω_{re}

The insights garnered from Table IV suggest that the frequency with which the parameter ω_{re} is updated exerts a negligible effect on both the wind energy capture efficiency and the drive-train loads. In fact, the historical cycle data are leveraged to guide the incremental adjustments of ω_{re} in the proposed adaptive algorithm for adjusting ω_{re} . Nevertheless, this technique falls short of pinpointing the quintessential parameters for optimal wind energy capture efficiency within discrete time frames. Therefore, it is evident that regardless of the variability in the update intervals of ω_{re} , P_{fav} is predominantly governed by different wind speeds.

Correspondingly, the narrow scope of fluctuation in ω_{re} signifies that any changes in update frequency are unlikely to produce marked consequences on the drive-train loads.

Based on the experiments, the following conclusions can be drawn.

TABLE IV
COMPARISON OF DIFFERENT UPDATE CYCLES OF CONTROL PERFORMANCE

\bar{v} (m/s)	Update cycle of ω_{re}	P_{avg} (%)	DEL
4	180	92.01	1.86
	360	92.24	1.85
	600	92.44	1.85
6	180	94.65	3.56
	360	94.87	3.55
	600	94.88	3.52

1) The results derived from experiments at variable wind speeds effectively validate the enhancement mechanism of the HOT method in terms of acceleration performance at different wind speeds.

2) The HOT method proposed in this paper substantially improves wind energy capture efficiency at variable wind speeds, and parameter ω_{re} can adaptively alter in line with the wind speed, demonstrating robust applicability.

3) The impact of parameter q on wind energy capture is deliberately excluded in this study and may be systematically investigated in subsequent control co-design research.

VI. CONCLUSION

Since the torque curve of the WTG using the existing DTG method augments the acceleration performance of WTGs, but fails to align optimally with the inherent aerodynamic torque characteristics of the WTG, its effect on enhancing wind energy capture efficiency is constrained. Hence, this study abandons the traditional quadratic function torque curve and proposes a MPPT control strategy based on a higher-order torque curve. The overarching objective of the proposed MPPT control strategy is to improve the acceleration performance of WTGs at different wind speeds, thereby enhancing the wind energy capture efficiency. Additionally, the torque command is succinct and possesses sound practical engineering application. However, the adjustment mechanism of the parameters within the torque curve is not adequately explored, serving as the focal point for further refinement of this study.

REFERENCES

- [1] S. Liu, C. Liu, Y. Wu *et al.*, "Tacholess order tracking method based on STFrFT for fault diagnosis of wind turbine gearbox under variable operating conditions," *IEEE Transactions on Instrumentation and Measurement*, vol. 73, p. 3513111, Mar. 2024.
- [2] Y. Chang, I. Kocar, J. Hu *et al.*, "Coordinated control of DFIG converters to comply with reactive current requirements in emerging grid codes," *Journal of Modern Power Systems and Clean Energy*, vol. 10, no. 2, pp. 502-514, Mar. 2022.
- [3] X. Tian, Y. Chi, P. Cheng *et al.*, "Dual-mode switching fault ride-through control strategy for self-synchronous wind turbines," *Journal of Modern Power Systems and Clean Energy*, vol. 11, no. 2, pp. 579-588, Mar. 2023.
- [4] J. Pande, P. Nasikkar, K. Kotecha *et al.*, "A review of maximum power point tracking algorithms for wind energy conversion systems," *Journal of Marine Science and Engineering*, vol. 9, no. 11, p. 1187, Oct. 2021.
- [5] A. Kushwaha, M. Gopal, and B. Singh, "Q-learning based maximum power extraction for wind energy conversion system with variable wind speed," *IEEE Transactions on Energy Conversion*, vol. 35, no. 3, pp. 1160-1170, Sept. 2020.
- [6] K. E. Johnson, L. J. Fingersh, M. J. Balas *et al.*, "Methods for increasing region 2 power capture on a variable-speed wind turbine," *Journal of Solar Energy Engineering*, vol. 126, no. 4, pp. 1092-1100, Nov. 2004.
- [7] D. Zouheyr, B. Lotfi, and B. Abdelmadjid, "Improved hardware implementation of a TSR based MPPT algorithm for a low cost connected wind turbine emulator under unbalanced wind speeds," *Energy*, vol. 232, p. 121039, Oct. 2021.
- [8] H. H. H. Mousa, A. R. Youssef, I. Hamdan *et al.*, "Performance assessment of robust P&O algorithm using optimal hypothetical position of generator speed," *IEEE Access*, vol. 9, pp. 30469-30485, Feb. 2021.
- [9] Y. Zou, M. E. Elbuluk, and Y. Sozer, "Stability analysis of maximum power point tracking (MPPT) method in wind power systems," *IEEE Transactions on Industry Applications*, vol. 49, no. 3, pp. 1129-1136, May 2013.
- [10] K. Yenduri and P. Sensarma, "Maximum power point tracking of variable speed wind turbines with flexible shaft," *IEEE Transactions on Sustainable Energy*, vol. 7, no. 3, pp. 956-965, Jul. 2016.
- [11] H. Chen, Y. Sun, Y. Cai *et al.*, "Improved torque compensation control based-maximum power point tracking strategy for large scale floating offshore wind turbines," *Ocean Engineering*, vol. 273, p. 113974, Apr. 2023.
- [12] K. E. Johnson, L. Y. Pao, M. J. Balas *et al.*, "Control of variable-speed wind turbines: standard and adaptive techniques for maximizing energy capture," *IEEE Control Systems Magazine*, vol. 26, no. 3, pp. 70-81, Jun. 2006.
- [13] M. Yin, X. Zhang, X. Ye *et al.*, "Improved MPPT control based on the reduction of tracking range," *Proceedings of the CSEE*, vol. 32, no. 27, pp. 24-31, Sept. 2012.
- [14] M. Yin, W. Li, C. Y. Chung *et al.*, "Optimal torque control based on effective tracking range for maximum power point tracking of wind turbines under varying wind conditions," *IET Renewable Power Generation*, vol. 11, no. 4, pp. 501-510, Mar. 2017.
- [15] J. Chen and Y. Song, "Dynamic loads of variable-speed wind energy conversion system," *IEEE Transactions on Industrial Electronics*, vol. 63, no. 1, pp. 178-188, Jan. 2016.
- [16] K. H. Kim, T. L. Van, D. C. Lee *et al.*, "Maximum output power tracking control in variable-speed wind turbine systems considering rotor inertial power," *IEEE Transactions on Industrial Electronics*, vol. 60, no. 8, pp. 3207-3217, Aug. 2013.
- [17] C. Pan and Y. Juan, "A novel sensorless MPPT controller for a high-efficiency microscale wind power generation system," *IEEE Transactions on Energy Conversion*, vol. 25, no. 1, pp. 207-216, Mar. 2010.
- [18] J. Chen, J. Chen, and C. Gong, "Constant-bandwidth maximum power point tracking strategy for variable-speed wind turbines and its design details," *IEEE Transactions on Industrial Electronics*, vol. 60, no. 11, pp. 5050-5058, Nov. 2013.
- [19] K. Johnson, L. Pao, M. Balas *et al.*, "Adaptive torque control of variable speed wind turbines," *IEEE Control Systems Magazine*, vol. 26, no. 3, pp. 70-81, Aug. 2004.
- [20] M. Hand, K. Johnson, L. Fingersh *et al.* (2004, May). Advanced control design and field testing for wind turbines at the national renewable energy laboratory. [Online]. Available: <https://www.nrel.gov/docs/fy04osti/36118.pdf>
- [21] X. Zhang, C. Huang, S. Hao *et al.*, "An improved adaptive-torque-gain MPPT control for direct-driven PMSG wind turbines considering wind farm turbulences," *Energies*, vol. 9, no. 11, p. 977, Nov. 2016.
- [22] X. Zhang, Y. Zhang, S. Hao *et al.*, "An improved maximum power point tracking method based on decreasing torque gain for large scale wind turbines at low wind sites," *Electric Power Systems Research*, vol. 176, p. 105942, Nov. 2019.
- [23] L. Guo, M. Yin, C. Cai *et al.*, "Optimal decreased torque gain control for maximizing wind energy extraction under varying wind speed," *Journal of Modern Power Systems and Clean Energy*, vol. 11, no. 3, pp. 853-862, May 2023.
- [24] B. Boukhezzer and H. Siguerdidjane, "Nonlinear control of a variable-speed wind turbine using a two-mass model," *IEEE Transactions on Energy Conversion*, vol. 26, no. 1, pp. 149-162, Mar. 2011.
- [25] H. Gu, Z. Chen, Q. Li *et al.*, "Active power control of wind turbine generators considering equilibrium point optimization under passive rotor speed variation mode," *IEEE Transactions on Sustainable Energy*, vol. 14, no. 4, pp. 2327-2337, Oct. 2023.
- [26] J. Mérida, L. T. Aguilar, and J. Dávila, "Analysis and synthesis of sliding mode control for large scale variable speed wind turbine for power optimization," *Renewable Energy*, vol. 71, pp. 715-728, Nov. 2014.
- [27] Z. Chen, M. Yin, Y. Zou *et al.*, "Maximum wind energy extraction for variable speed wind turbines with slow dynamic behavior," *IEEE*

- Transactions on Power Systems*, vol. 32, no. 4, pp. 3321-3322, Jul. 2017.
- [28] L. Zhou, M. Yin, X. Sun *et al.*, "Maximum power point tracking control of wind turbines based on equivalent sinusoidal wind," *Electric Power Systems Research*, vol. 223, p. 109534, Oct. 2023.
- [29] Y. Wang, J. Meng, X. Zhang *et al.*, "Control of PMSG-based wind turbines for system inertial response and power oscillation damping," *IEEE Transactions on Sustainable Energy*, vol. 6, no. 2, pp. 565-574, Apr. 2015.
- [30] M. Yin, W. Li, C. Y. Chung *et al.*, "Inertia compensation scheme of WTS considering time delay for emulating large-inertia turbines," *IET Renewable Power Generation*, vol. 11, no. 4, pp. 529-538, Mar. 2017.
- [31] W. Li, M. Yin, Z. Chen *et al.*, "Inertia compensation scheme for wind turbine simulator based on deviation mitigation," *Journal of Modern Power Systems and Clean Energy*, vol. 5, no. 2, pp. 228-238, Mar. 2017.
- [32] J. M. Jonkman and M. L. Buhl (2005, Oct.). FAST user's guide. [Online]. Available: <https://www.nrel.gov/docs/fy06osti/38230.pdf>
- [33] Q. Yao, B. Ma, T. Zhao *et al.*, "Optimized active power dispatching of wind farms considering data-driven fatigue load suppression," *IEEE Transactions on Sustainable Energy*, vol. 14, no. 1, pp. 371-380, Jan. 2023.
- [34] E. A. Bossanyi. (2017, Jul.). GH bladed theory manual. [Online]. Available: <https://kupdf.net/download/gh-bladed-theorymanual596b5c9bdc0d60d422a88e79.pdf>

Liansong Guo received the B.S. degree in mathematics from Nanjing University of Science and Technology, Nanjing, China, in 2018. He is currently working toward the Ph.D. degree in control science and engineering with the School of Automation, Nanjing University of Science and Technology. His research interest includes wind turbine control.

Zaiyu Chen received the B.S. degree in information and computing science and the Ph.D. degree in control science and engineering from the Nanjing

University of Science and Technology, Nanjing, China, in 2012 and 2019, respectively. From 2020 to 2021, he was a Research Fellow with the School of Electrical and Electronic Engineering, Nanyang Technological University, Singapore. He is currently a Lecturer with the School of Automation, Nanjing University of Science and Technology. His research interests include active power control for wind turbines and its application in power system frequency regulation.

Minghui Yin received the B.Eng. and M.Eng. degrees in electrical power engineering and the Ph.D. degree in control science and engineering from Nanjing University of Science and Technology, Nanjing, China, in 1999, 2002, and 2009, respectively. From 2007 to 2008, he was a Research Assistant with the Department of Electrical Engineering, The Hong Kong Polytechnic University, Hong Kong, China. From 2016 to 2017, he was a Visiting Scholar with the School of Electrical and Information Engineering, The University of Sydney, Sydney, Australia. He is currently a Professor with the School of Automation, Nanjing University of Science and Technology. His main research interests include wind power conversion system and transient stability of power system.

Chenxiao Cai received the Ph.D. degree in control science and engineering from Nanjing University of Science and Technology, Nanjing, China, in 2005. She is currently a Professor with the School of Automation, Nanjing University of Science and Technology. Her main research interests include singularly perturbed system, singular system, robust control, unmanned aerial vehicle, and deep learning algorithm.

Yun Zou received the B.S. degree in mathematics from Northwestern University, Xi'an, China, in 1983, and the M.S. and Ph.D. degrees in control theory and control engineering from Nanjing University of Science and Technology, Nanjing, China, in 1987 and 1990, respectively. He is currently a Professor with the School of Automation, Nanjing University of Science and Technology. His current research interests include differential-algebraic equation system, two-dimensional system, singular perturbation, transient stability of power system, and electricity market.